

Telerehabilitation Through a Remotely Operated Motorized Functional Electric Stimulation Actuated Cycle

Kimberly J. Stubbs¹, Brendon C. Allen², *Member, IEEE*, and Warren E. Dixon¹, *Fellow, IEEE*

Abstract—Neuromuscular disorders (NDs) affect millions of people each year, many of whom are prescribed functional electrical stimulation (FES) rehabilitative cycling. However, it is often difficult for many with NDs to attend regularly scheduled physical therapy sessions, a fact which is exasperated by the ongoing COVID-19 pandemic. This article details the development of a teleoperated FES-actuated rehabilitation system for two use cases: a remote physical therapy session for people not able to attend in person, and a rehab-by-wire style system where the rehabilitation participant sets the desired trajectory of the FES-actuated lower-body cycle using a motorized hand-cycle, thus coordinating the upper and lower limbs. In both cases, the lower-body rehabilitation cycle has a split-crank to capture asymmetries in lower-body performance. Lyapunov-based analysis methods are used to prove global exponential tracking to the desired position and cadence determined by the master-cycle system. Five people were tested for each use case, where the teleoperated FES-actuated rehabilitative lower-body cycling system resulted in an average rms position error (calculated across both use cases) of 6.14° and an average rms cadence error of 3.77 RPM, despite an unpredictable, variable desired cadence. The calculated average position error was found to be $0.04^\circ \pm 5.96^\circ$, thus eliminating undesirable steady-state position errors reported in prior works.

Index Terms—Functional electrical stimulation (FES), physical human-machine interaction, rehab-by-wire, rehabilitation robotics, teleoperation, telerehabilitation.

I. INTRODUCTION

SIGNIFICANT motivation exists for the development of remotely provided healthcare solutions, fueled by the ongoing COVID-19 pandemic, a desire to protect those who are immunocompromised, and the lack of care for people who reside in rural communities. Recent advancements have

Manuscript received 8 January 2022; revised 13 July 2023; accepted 29 October 2023. Date of publication 14 December 2023; date of current version 25 April 2024. This work was supported in part by NSF under Award 1762829, in part by the Assistant Secretary of Defense for Health Affairs, through the Congressionally Directed Medical Research Program under Award W81XWH1910330, and in part by the National Defense Science and Engineering Graduate Fellowship Program. Recommended by Associate Editor A. Macchelli. (*Corresponding author: Kimberly J. Stubbs.*)

This work involved human subjects or animals in its research. Approval of all ethical and experimental procedures and protocols was granted by the Institutional Review Board at the University of Florida.

Kimberly J. Stubbs and Warren E. Dixon are with the Department of Mechanical and Aerospace Engineering, University of Florida, Gainesville, FL 32611 USA (e-mail: kimberlyjstubbs@ufl.edu; wdixon@ufl.edu).

Brendon C. Allen is with the Department of Mechanical Engineering, Auburn University, Auburn, AL 36849 USA (e-mail: bca0027@auburn.edu). Digital Object Identifier 10.1109/TCST.2023.3338815

led to online access to some medical care, but options are limited for those who require regular rehabilitation [1]. One commonly prescribed rehabilitation method for people with neuromuscular disorders (NDs) is functional electrical stimulation (FES), where muscle contractions are induced through the application of an electric field across a targeted muscle group for the purpose of completing a functional task, such as pedaling an ergometer [2], [3]. FES rehabilitation has been shown to have multiple health benefits, including improved muscle strength [4], increased range of motion [5], improved cardiovascular health [6], increased bone density [7], and restoration of motor control [8], [9]. Therefore, the authors are motivated to design and develop FES remote rehabilitation solutions for people with NDs.

Robotic end-effectors and exoskeletons have been used to provide assistance during rehabilitation and recovery [10], where, in many cases, this robotic intervention has been shown to improve therapeutic outcomes [11] and can significantly increase the speed of motor recovery for people who have experienced a stroke [12]. FES/motor actuated recumbent cycles can be expected to provide substantial rehabilitative benefit. However, according to Molteni et al. [10], an ideal rehabilitative robotic device should “ensure early, intensive, task-specific, and multisensory stimulations.” Therefore, further motivation exists to ensure FES rehabilitative cycling devices are capable of inducing intensive and task-oriented performance by the rehabilitation participant while also introducing multisensory feedback. It has been shown in studies on neuroplasticity that repetitive physical exercise alone is unlikely to restore motor function [13], and that the addition of sensory inputs, such as visual stimulation, kinematic feedback, or other cognitive enhancements, is likely to generate reactivation of neural pathways within the brain [14].

Recent works have used constructive (Lyapunov-based) analysis-based design methods to adapt to unknown system parameters and nonlinear dynamics inherent to FES-actuated cycling [15], and have introduced switching between FES-induced muscle effort and electric motor effort, thereby extending the duration of FES rehabilitation sessions by avoiding uncomfortable over stimulation and early onset of muscle fatigue [16]. Some studies have shown that matching the positions of the upper and lower limbs by using a mechanically coupled cycle can improve walking for stroke patients [17].

This result supports the suggestion that neural connections exist between the lower and upper limbs [18]. Efforts have been made to produce a commercially available solution to allow for recurring FES cycling combined with a mechanically coupled hand-cycle (e.g., the BerkelBike). However, such systems do not ensure that the upper and lower limbs are consistently in paired positions (i.e., the crank position of the lower limb matches the corresponding upper limb crank position) as suggested in [17]. A recent study specific to FES rehabilitation enforced paired positioning between the limbs by simultaneously stimulating the arms and legs while pedaling mechanically coupled cycles, resulting in a significant improvement in both walking distance and pace [19].

Planned, repetitive movement can also lead to motor recovery [20] when the movement is designed to be enjoyable for the participant, leading to an improved emotional and physical state [21]. Successful rehabilitation for those with NDs is a long process, including regular weekly or daily at-home rehabilitation exercise regimes, as well as regular visits with a physical therapist [22]. Unfortunately, many participants find that the repetitive nature of their exercise routines do not provide sufficient motivation to continue prescribed treatments. Therefore, significant research effort has been devoted to the development of game-based, teleoperative rehabilitative systems [22], [23], [24]. While these systems are capable of directing the rehabilitation participant's desired trajectories as set by a teleoperated master-cycle (i.e., a cycle operated by a remotely located physical therapist) [25], [26], [27], they do not include kinematic feedback to inform the master-cycle operator of the rehabilitation participant's current cadence and position. Thus, strong motivation exists to build on the results detailed above by developing advanced FES rehabilitation systems to fulfill the needs of multiple use cases.

One important use case is to enable physical therapists to provide teleoperated remote therapy sessions for people with NDs. In this case, for the purpose of this article, the teleoperation master-cycle is a recumbent single-crank cycle with similar dynamics to the FES rehabilitation cycle. Here, a motor is used only to provide kinematic feedback, as depicted in Fig. 1. This use case, hereafter referred to as telerehabilitation,¹ allows the therapist to synchronize with the rehabilitation participant and receive physical feedback related to their performance. Telerehabilitation could prove invaluable to people who are unable to participate in on-site rehabilitation sessions. In a second use case, where a rehabilitation participant may be asked to complete ongoing treatment in their home, a system capable of pairing the position between corresponding upper and lower limbs of the rehabilitative participant as in [17] and [19] is desirable. Further benefit would be provided with the inclusion of added sensory inputs and by increasing cognitive direction of performance (i.e., allowing the rehabilitation participant

¹This work presents a development across multiple use cases, some of which are not typically affected by communication delays. Therefore, the existence of communication delays common to teleoperated systems has been neglected. The subsequent Discussion section addresses communication delays in current works on FES telerehabilitation [28].



Fig. 1. Remotely operated FES-actuated split-crank telerehabilitation system shown in the foreground, where the desired position and cadence are set by a separate operator on a single-crank recumbent cycle shown in the background. Forward rotation of the crank arm, subsequently referenced in the control development, is that which would produce forward movement of the cycle if it were not stationary.



Fig. 2. Rehab-by-wire style teleoperated FES-actuated split-crank rehabilitation system, where the desired position and cadence are set by the user-operated hand-cycle marked by the letter A. The stimulation unit and dermal stimulation pads are marked by the letter B. The split-crank recumbent cycle crank sets are marked by the letter C.

to set the desired trajectory of the FES-actuated lower-limb cycle using an upper-limb cycle). This second use case, hereafter referred to as rehab-by-wire (so-called based on the popular drive-by-wire concepts in results such as [29], [30], and [31]), is likely to make the rehabilitative experience more enjoyable, thus motivating the completion of prescribed treatments. Rehab-by-wire systems would also open the door to the possibility of “game-ified” rehabilitation sessions, further increasing participant enjoyment and motivation. The rehab-by-wire master-cycle used in this publication consists of a hand-powered wheel, where no mechanical coupling exists between the master and leader cycles, and an in-line motor is used to provide kinematic feedback to the operator, as depicted in Fig. 2.

This article is an extension of the authors' recently developed bilateral teleoperated FES rehabilitation system in [32],

where the FES muscle and motor controllers were developed to track a master-cycle trajectory and the Lyapunov analysis proved global exponential stability. In the current publication, testing and validation is performed using a split-crank cycle (i.e., a cycle where the left and right crank arms can independently drive the system) which serves as the rehabilitation follower-cycle (i.e., the system whose control effort is designed to track the trajectory of a master-cycle). The purpose of using a split-crank cycle is to isolate and capture any asymmetries in impairment. Furthermore, no mechanical coupling exists between the master-cycle and rehabilitative lower-body cycle, such that any torque applied to the follower-cycle is provided by the rehabilitation participant's muscle effort or by the motor when muscle effort is not sufficient to track the desired master-cycle trajectory. Prior works have typically focused on providing accurate cadence tracking, often leading to substantial steady-state position error. Such errors could lead to inaccurate application of feedback to the operator during telerehabilitation or reduced rehabilitative benefit during rehab-by-wire. Therefore, in this work, emphasis is placed on accurate position tracking, leading to the addition of an integral term for the position error. Five non-disabled participants were tested for both the telerehabilitation and rehab-by-wire use cases. The FES-actuated telerehabilitation lower-body cycling system resulted in an average rms position error (calculated across both use cases) of 6.14° and an average rms cadence error of 3.77 RPM, despite an unpredictable, variable desired cadence. The calculated average position error was found to be $0.04^\circ \pm 5.96^\circ$, thus eliminating the steady-state position error previously reported when operating a split-crank cycle [33], [34].

II. DYNAMIC MODELS

A. Rehabilitative Lower-Body Cycling System

A split-crank rehabilitative cycle, where each crank arm is capable of driving the cycle independently as detailed in [33] and [35], was used to account for asymmetries by decoupling the legs (i.e., the dynamics associated with a single-side crank set is modeled as an independent system). The cycle-rider lower body (i.e., follower) dynamics for one side are modeled as [35]

$$\tau_{e_l} = \tau_{c_l}(q_l, \dot{q}_l, \ddot{q}_l, t) + \tau_{r_l}(q_l, \dot{q}_l, \ddot{q}_l, t) \quad (1)$$

where $q_l: \mathbb{R}_{\geq 0} \rightarrow \mathcal{Q}_l$ denotes the angular position, and $\mathcal{Q}_l \subseteq \mathbb{R}$ is the set of all possible measurable lower-body cycle crank angles. The measurable angular velocity (cadence) of the lower-body cycle crank arm is denoted by $\dot{q}_l: \mathbb{R}_{\geq 0} \rightarrow \mathbb{R}$, and the unmeasurable angular acceleration is denoted by $\ddot{q}_l: \mathbb{R}_{\geq 0} \rightarrow \mathbb{R}$. In (1), $\tau_{e_l}: \mathcal{Q}_l \times \mathbb{R} \times \mathbb{R} \times \mathbb{R}_{\geq 0} \rightarrow \mathbb{R}$ represents the electric motor torque, $\tau_{c_l}: \mathcal{Q}_l \times \mathbb{R} \times \mathbb{R} \times \mathbb{R}_{\geq 0} \rightarrow \mathbb{R}$ represents the cycle torque, and $\tau_{r_l}: \mathcal{Q}_l \times \mathbb{R} \times \mathbb{R} \times \mathbb{R}_{\geq 0} \rightarrow \mathbb{R}$ represents the rider torque. The rider torque in (1) can be divided into

$$\tau_{r_l}(q_l, \dot{q}_l, \ddot{q}_l, t) \triangleq \tau_{p_l}(q_l, \dot{q}_l, \ddot{q}_l) - \tau_M(q_l, \dot{q}_l, t) + d_{r_l}(t) \quad (2)$$

where the passive forces (i.e., no muscle effort applied) are denoted by $\tau_{p_l}: \mathcal{Q}_l \times \mathbb{R} \times \mathbb{R} \rightarrow \mathbb{R}$, the torques produced by muscle forces are denoted by $\tau_M: \mathcal{Q}_l \times \mathbb{R} \times \mathbb{R}_{\geq 0} \rightarrow \mathbb{R}$, and rider disturbances are denoted by $d_{r_l}: \mathbb{R}_{\geq 0} \rightarrow \mathbb{R}$. Substituting (2) into (1), and following the method of development in [32], the combined lower-body rehabilitation cycle-rider dynamics are expressed by²

$$\tau_M + \tau_{e_l} = M_l \ddot{q}_l + \frac{1}{2} \dot{M}_l \dot{q}_l + G_l + P_l + b_{c_l} \dot{q}_l + d_{c_l} + d_{r_l} \quad (3)$$

where $M_l: \mathcal{Q}_l \rightarrow \mathbb{R}$, $(1/2)\dot{M}_l: \mathcal{Q}_l \times \mathbb{R} \rightarrow \mathbb{R}$, $G_l: \mathcal{Q}_l \rightarrow \mathbb{R}$, $P_l: \mathcal{Q}_l \times \mathbb{R} \rightarrow \mathbb{R}$, and $b_{c_l} \in \mathbb{R}_{\geq 0}$ represent the unknown, nonlinear inertial effects, centripetal-Coriolis effects, gravitational effects, passive viscoelastic muscle forces, and viscous damping of the cycle, respectively. The cycle and rider disturbances are denoted by $d_{c_l}: \mathbb{R}_{\geq 0} \rightarrow \mathbb{R}$ and $d_{r_l}: \mathbb{R}_{\geq 0} \rightarrow \mathbb{R}$. The muscle torques in (3) are modeled as the summation across all FES induced muscle forces plus any volitional efforts of the rider, denoted by $\tau_{vol_l} \in \mathbb{R}_{\geq 0}$, such that [36]

$$\tau_M = \sum_{m \in \mathcal{M}} B_{m_l}(q_l, \dot{q}_l) u_{m_l}(q_l, t) + \tau_{vol_l} \quad (4)$$

where the subscript $m \in \mathcal{M} = \{Q, G, H\}$ indicates the quadriceps femoris (Q), gluteal (G), and hamstring (H) muscle groups. The nonlinear, unknown muscle control effectiveness is denoted by $B_{m_l}: \mathcal{Q}_l \times \mathbb{R} \rightarrow \mathbb{R}_{\geq 0}$, $\forall m \in \mathcal{M}$ and the designed FES muscle control input (i.e., pulsewidth) is denoted by $u_{m_l}: \mathcal{Q}_l \times \mathbb{R}_{\geq 0} \rightarrow \mathbb{R}$. The subset $\mathcal{Q}_m \subset \mathcal{Q}_l$, $\forall m \in \mathcal{M}$, where a given muscle group receives stimulation, is determined as in [33]

$$\mathcal{Q}_m \triangleq \{q_l \in \mathcal{Q}_l \mid T_m(q_l) > \varepsilon_m\} \quad (5)$$

where $\varepsilon_m \in [0, \max(T_m)]$ represents a user-defined lower limit for each muscle group's torque transfer ratio, $T_m: \mathcal{Q}_l \rightarrow \mathbb{R}$, to ensure that any muscle effort resulting from stimulation only produces positive crank rotation. The region about the crank cycle where FES produces a positive crank torque is denoted by $\mathcal{Q}_{FES} \triangleq \cup_{m \in \mathcal{M}} \{\mathcal{Q}_m\}$, $\forall m \in \mathcal{M}$.

The muscle control input for each muscle group is defined as $u_m \triangleq \sigma_m(q_l) k_m u_s(t)$, $\forall m \in \mathcal{M}$, where $k_m \in \mathbb{R}_{\geq 0}$ is a selectable constant chosen to guarantee participant comfort during muscle stimulation, $u_s(t)$ represents the subsequently designed FES control input, and σ_m denotes a switching signal determined using (5), where $\sigma_m: \mathcal{Q}_l \rightarrow \{0, 1\}$ such that

$$\sigma_m \triangleq \begin{cases} 1, & \text{if } q_l \in \mathcal{Q}_m \\ 0, & \text{if } q_l \notin \mathcal{Q}_m. \end{cases} \quad (6)$$

The electric motor torque produced about the leg-cycle crank axis is expressed as follows:

$$\tau_{e_l} \triangleq B_{e_l} u_{e_l}(t) \quad (7)$$

where $B_{e_l} \in \mathbb{R}_{\geq 0}$ represents the nonlinear, unknown relationship between the electric motor current and the resulting torque about the crank axis. The subsequently designed leg-cycle motor control input is represented by $u_{e_l}(t)$.

²Here, and throughout the remaining text, functional dependencies are removed for brevity, except where required for added clarity.

Substituting (4) and (7) into (3), and combining the individual muscle torque efficiencies such that $B_M \triangleq \sum_{m \in \mathcal{M}} B_m \sigma_m k_m$, produces

$$B_M u_s + B_{e_l} u_{e_l} = M_l \ddot{q}_l + \frac{1}{2} \dot{M}_l \dot{q}_l + G_l + P_l + b_{c_l} \dot{q}_l + d_{c_l} + d_{r_l} - \tau_{\text{vol}_l}. \quad (8)$$

B. Master-Cycle System

The master-cycle dynamics for both use cases (i.e., telerehabilitation and rehab-by-wire) are modeled as follows:

$$\tau_{e_{\text{mc}}} \triangleq \tau_{c_{\text{mc}}}(q_{\text{mc}}, \dot{q}_{\text{mc}}, \ddot{q}_{\text{mc}}, t) + \tau_{r_{\text{mc}}}(q_{\text{mc}}, \dot{q}_{\text{mc}}, \ddot{q}_{\text{mc}}, t) \quad (9)$$

where $q_{\text{mc}}: \mathbb{R}_{\geq 0} \rightarrow \mathcal{Q}_{\text{mc}}$, denotes the angular position of the master-cycle crank, and $\mathcal{Q}_{\text{mc}} \subseteq \mathbb{R}$ represents the set of all possible measurable master-cycle crank angles. The measured angular velocity and the unmeasurable angular acceleration of the master-cycle system are denoted by $\dot{q}_{\text{mc}}: \mathbb{R}_{\geq 0} \rightarrow \mathbb{R}$ and $\ddot{q}_{\text{mc}}: \mathbb{R}_{\geq 0} \rightarrow \mathbb{R}$, respectively. Following the same process as shown for the lower-body cycling system, and recognizing that the forces applied by the rider about the master-cycle crank axis, denoted by $\tau_{\text{vol}_{\text{mc}}} \in \mathbb{R}_{\geq 0}$, are purely volitional, the master-cycle system in (9) can be expressed as follows:

$$B_{e_{\text{mc}}} u_{e_{\text{mc}}} + \tau_{\text{vol}_{\text{mc}}} = M_{\text{mc}} \ddot{q}_{\text{mc}} + \frac{1}{2} \dot{M}_{\text{mc}} \dot{q}_{\text{mc}} + G_{\text{mc}} + P_{\text{mc}} + b_{c_{\text{mc}}} \dot{q}_{\text{mc}} + d_{\text{mc}} \quad (10)$$

where $B_{e_{\text{mc}}} \in \mathbb{R}_{\geq 0}$ represents the nonlinear, unknown relationship between the electric motor current and the resulting torque about the master-cycle crank axis. The subsequently designed master-cycle motor control input is represented by $u_{e_{\text{mc}}}(t)$. The nonlinear, unknown inertial effects, gravitational effects, passive viscoelastic muscle forces, and viscous damping in (10) are represented by $M_{\text{mc}}: \mathcal{Q}_{\text{mc}} \rightarrow \mathbb{R}$, $G_{\text{mc}}: \mathcal{Q}_{\text{mc}} \rightarrow \mathbb{R}$, $P_{\text{mc}}: \mathcal{Q}_{\text{mc}} \times \mathbb{R} \rightarrow \mathbb{R}$, and $b_{c_{\text{mc}}} \in \mathbb{R}_{\geq 0}$, respectively. The lumped unknown cycle and rider disturbances for the master-cycle system is denoted by d_{mc} , where $d_{\text{mc}} = d_{c_{\text{mc}}} + d_{r_{\text{mc}}}$.

C. System Properties

The lower-body rehabilitative cycling system in (8) and the master-cycle system in (10) have the following properties and assumptions, where $i = \{l, \text{mc}\}$ [16].

Property 1: $c_{m_i} \leq M_i \leq c_{M_i}$ where $c_{m_i}, c_{M_i} \in \mathbb{R}_{\geq 0}$ are known constants.

Property 2: $|(1/2)\dot{M}_i| \leq c_{V_i} |\dot{q}_i| \in \mathbb{R}_{\geq 0}$ where c_{V_i} is a known constant.

Property 3: $|G_i| \leq c_{G_i} \in \mathbb{R}_{\geq 0}$ where c_{G_i} is a known constant.

Property 4: $|P_i| \leq c_{P1_i} + c_{P2_i} |\dot{q}_i|$ where $c_{P1_i}, c_{P2_i} \in \mathbb{R}_{\geq 0}$ are known constants.

Property 5: $|b_{c_i}| \leq c_{b_i}$ where $c_{b_i} \in \mathbb{R}_{\geq 0}$ is a known constant.

Property 6: $|d_{c_i} + d_{r_i}| \leq c_{d_i} \in \mathbb{R}_{\geq 0}$ where c_{d_i} is a known constant.

Property 7: $B_{e_i} \leq B_{e_l} \leq B_{e_r}$ where $B_{e_l}, B_{e_r} \in \mathbb{R}_{>0}$.

Property 8: The combined muscle efficiency B_M has a lower bound as in [36] such that when $\sum_{m \in \mathcal{M}} \sigma_m > 0$, $B_M \leq B_M$ where $B_M \in \mathbb{R}_{>0}$.

Assumption 1: Physical limitations dictate that q_{mc} is sufficiently smooth (i.e., $q_{\text{mc}}, \dot{q}_{\text{mc}}, \ddot{q}_{\text{mc}} \in \mathcal{L}_{\infty}$) and that the volitional torques produced by the rehabilitation participant and master-cycle operator are upper bounded such that $|\tau_{\text{vol}_i}| \leq c_{\text{vol}_i} \in \mathbb{R}_{\geq 0}$.

III. CONTROL DEVELOPMENT

A strongly coupled telerobotic system [37] is developed, where the desired angular position tracked by the FES/motor actuated lower-body cycling system is defined as the master-cycle position. To ensure accurate position tracking, an integral of the position error, denoted by $e_0: \mathbb{R}_{\geq 0} \rightarrow \mathbb{R}$, and two auxiliary errors, denoted by $e_1: \mathbb{R}_{\geq 0} \rightarrow \mathbb{R}$ and $r: \mathbb{R}_{\geq 0} \rightarrow \mathbb{R}$, are defined as follows:

$$e_0 \triangleq \int_{t_0}^t (q_{\text{mc}}(s) - q_l(s)) ds \quad (11)$$

$$e_1 \triangleq \dot{e}_0 + \alpha_0 e_0 \quad (12)$$

$$r \triangleq \dot{e}_1 + \alpha_1 e_1 \quad (13)$$

where $\alpha_0, \alpha_1 \in \mathbb{R}_{\geq 0}$ are selectable constants.

Taking the time derivative of (13), multiplying by M_l , substituting in (11)–(13), and rearranging yields

$$M_l \dot{r} = M_l [\ddot{q}_{\text{mc}} - \ddot{q}_l + (\alpha_0 + \alpha_1)(r - \alpha_1 e_1) - \alpha_0^2 (e_1 - \alpha_0 e_0)]. \quad (14)$$

The dynamics of the lower-body and master-system cycles can be incorporated by rearranging (8) and (10), substituting into (14) for \ddot{q}_l and \ddot{q}_{mc} , and performing some algebraic manipulation to yield

$$M_l \dot{r} = \chi - \frac{1}{2} \dot{M}_l r - e_1 - B_M u_s - B_{e_l} u_{e_l} + M_l M_{\text{mc}}^{-1} B_{e_{\text{mc}}} u_{e_{\text{mc}}} \quad (15)$$

where the auxiliary term $\chi: \mathbb{R} \times \mathbb{R} \times \mathbb{R}_{\geq 0} \rightarrow \mathbb{R}$ is defined as follows:

$$\begin{aligned} \chi \triangleq M_l & \left[(\alpha_0 + \alpha_1)r - (\alpha_0 + \alpha_1)^2 e_1 + \alpha_0^3 e_0 + \alpha_0 \alpha_1 e_1 \right. \\ & \left. + M_{\text{mc}}^{-1} \left(-\frac{1}{2} \dot{M}_{\text{mc}} \dot{q}_{\text{mc}} - G_{\text{mc}} \right. \right. \\ & \left. \left. - b_{c_{\text{mc}}} \dot{q}_{\text{mc}} - P_{\text{mc}} - d_{\text{mc}} + \tau_{\text{vol}_{\text{mc}}} \right) \right] \\ & + \frac{1}{2} \dot{M}_l [\dot{q}_{\text{mc}} + (\alpha_0 + \alpha_1)e_1 - \alpha_0^2 e_0] \\ & + b_{c_l} [\dot{q}_{\text{mc}} - r + (\alpha_0 + \alpha_1)e_1 - \alpha_0^2 e_0] \\ & + d_{c_l} + G_l + P_l + d_{r_l} + e_1 - \tau_{\text{vol}_l}. \end{aligned}$$

From Properties 1–6 and Assumption 1, χ can be upper bounded as follows:

$$|\chi| \leq c_1 + c_2 \|z\| + c_3 \|z\|^2 \quad (16)$$

where $z \in \mathbb{R}^3$ is defined as $z \triangleq [e_0 \ e_1 \ r]^T$, and $c_1, c_2, c_3 \in \mathbb{R}_{\geq 0}$ are known constants.

From (13), (15), and the subsequent stability analysis, the FES control input is designed as follows:

$$u_s = \sigma_s (k_1 r + [k_2 + k_3 \|z\| + k_4 \|z\|^2] \text{sgn}(r)) \quad (17)$$

where $k_1, k_2, k_3, k_4 \in \mathbb{R}_{\geq 0}$ are selectable constant control gains and the switching signal, $\sigma_s: \mathcal{Q}_l \rightarrow \{0, 1\}$, for lower-body muscle stimulation is designed as follows:

$$\sigma_s \triangleq \begin{cases} 1, & \text{if } q_l \in \mathcal{Q}_{\text{FES}} \\ 0, & \text{if } q_l \notin \mathcal{Q}_{\text{FES}}. \end{cases} \quad (18)$$

It has been previously shown in [33] and [34] that maintaining accurate position tracking can be challenging when operating a split-crank rehabilitation cycle, particularly in the hamstring stimulation region, where $q_l \in \mathcal{Q}_H$, due to the lack of agonist muscle torques typically produced by the quadriceps femoris muscle group of the opposing leg on a standard joined-crank cycle. The lack of assistive effort leads to saturated stimulation levels in weaker muscle groups, causing poor tracking, muscle fatigue, and participant discomfort. Motivated by the desire to provide motor-actuated assistive torque as needed, from (13) and (15), and the subsequent stability analysis, the lower-body motor control input is designed as follows:

$$u_{e_l} = \sigma_e (k_5 r + [k_6 + k_7 \|z\| + k_8 \|z\|^2] \text{sgn}(r)) \quad (19)$$

where $k_5, k_6, k_7, k_8 \in \mathbb{R}_{\geq 0}$ are selectable constant control gains.³ A discontinuous switching signal for lower-body motor assistance, $\sigma_e: \mathcal{Q}_l \times \{0, 1\} \rightarrow [0, 1]$, is defined as follows:

$$\sigma_e \triangleq \prod_{m \in \mathcal{M}} (1 - \beta_m \sigma_m) \quad (20)$$

where $\beta_m \in [0, 1]$, for all $m \in \mathcal{M}$ are selectable constants to vary the motor current applied within each FES region. In the case where $\sigma_m = 0$, for all $m \in \mathcal{M}$ (i.e., when $q_l \notin \mathcal{Q}_{\text{FES}}$), $\sigma_e = 1$.

To ensure only resistive application of motor effort is applied to the master-cycle system, thus providing informative kinematic feedback to the operator, a switching signal, $\sigma_{mc}: \mathbb{R} \times \mathbb{R} \rightarrow \{0, 1\}$, is designed as follows:

$$\sigma_{mc} \triangleq \begin{cases} 1, & \text{if } \dot{q}_{mc} \dot{e}_0 > 0 \\ 0, & \text{if } \dot{q}_{mc} \dot{e}_0 \leq 0. \end{cases} \quad (21)$$

In the case that the master-cycle system is operating in forward rotation ($\dot{q}_{mc} > 0$) and the lower-body angular position of the legs is less than the angular position of the master-cycle (i.e., the instantaneous position error is positive such that $\dot{e}_0 > 0$), or where the master-cycle is operating with reversed rotation ($\dot{q}_{mc} < 0$) and the lower-body angular position is larger than that of the master-cycle ($\dot{e}_0 < 0$), then $\sigma_{mc} = 1$ and opposing motor effort will be applied about the master-cycle crank. However, in the case where $\dot{q}_{mc} > 0$, and the lower-body position has overshoot the master-cycle such that $\dot{e}_0 < 0$, then $\sigma_{mc} = 0$ and the master-cycle operator will experience no resistive or assistive efforts. The master-cycle position-error feedback motor controller is designed as follows:

$$u_{e_{mc}} = -k_9 \sigma_{mc} \dot{e}_0. \quad (22)$$

³In general, the use of multiple sliding mode controllers can induce chatter. The experimental data in this case, where the control efforts are proportional when simultaneously applied, indicates minimal high frequency components. However, effort will be made in future works to eliminate the use of a dual sliding mode controller.

Substituting (17), (19), and (22) into (15) produces the closed-loop error system

$$\begin{aligned} M_l \dot{r} = & \chi - \frac{1}{2} \dot{M}_l r - e_1 - B_M \sigma_s k_1 r - B_{e_l} \sigma_e k_5 r \\ & - B_M \sigma_s [k_2 + k_3 \|z\| + k_4 \|z\|^2] \text{sgn}(r) \\ & - B_{e_l} \sigma_e [k_6 + k_7 \|z\| + k_8 \|z\|^2] \text{sgn}(r) \\ & - M_l M_{mc}^{-1} B_{e_{mc}} \sigma_{mc} k_9 \dot{e}_0. \end{aligned} \quad (23)$$

IV. STABILITY ANALYSIS

A Lyapunov-based stability analysis is provided for two cases; when $q_l \notin \mathcal{Q}_{\text{FES}}$ and when $q_l \in \mathcal{Q}_{\text{FES}}$. Switching times between cases are denoted by $\{t_n^i\}$, $i \in \{e, s\}$, $n \in \{0, 1, 2, \dots\}$ where each t_n^i represents the n -th time that the lower-body rehabilitation cycle switches to the electric motor only region (denoted by $i = e$) or to the stimulation region (denoted by $i = s$). For the master-cycle system (i.e., the teleoperation controller) stability analysis, it is also shown that all system states are bounded [37].

Theorem 1: For $q_l \notin \mathcal{Q}_{\text{FES}}$, where $t \in [t_n^e, t_n^s)$, the position and cadence error systems are globally exponentially stable in the sense that

$$\|z(t)\| \leq \sqrt{\frac{\lambda_2}{\lambda_1}} \|z(t_n^e)\| \exp\left[-\frac{\min(\psi_1, \psi_2, \psi_3)}{2\lambda_2} (t - t_n^e)\right] \quad (24)$$

provided the following gain conditions are met:

$$k_6 > \frac{c_1}{B_{e_l}}, \quad k_7 > \frac{c_2}{B_{e_l}}, \quad k_8 > \frac{c_3}{B_{e_l}} \quad (25)$$

$$k_5 > \frac{B_{e_{mc}}}{2B_{e_l}} \frac{c_{M_l}}{c_{m_{mc}}} k_9 (1 + \alpha_0) \quad (26)$$

$$\alpha_1 > \frac{1}{2} \left(1 + \frac{c_{M_l}}{c_{m_{mc}}} B_{e_{mc}} k_9 \right) \quad (27)$$

$$\alpha_0 > \frac{c_{m_{mc}}}{2c_{m_{mc}} - c_{M_l} B_{e_{mc}} k_9} \quad (28)$$

$$k_9 < \frac{2c_{m_{mc}}}{c_{M_l} B_{e_{mc}}} \quad (29)$$

where ψ_1, ψ_2, ψ_3 are known positive constants that can be adjusted through user-defined control gains.

A positive definite, radially unbounded, common Lyapunov function candidate, $V: \mathbb{R} \rightarrow \mathbb{R}_{\geq 0}$, is defined as follows:

$$V = \frac{1}{2} M_l r^2 + \frac{1}{2} e_1^2 + \frac{1}{2} e_0^2 \quad (30)$$

such that

$$\lambda_1 \|z\|^2 \leq V \leq \lambda_2 \|z\|^2 \quad (31)$$

where $\lambda_1 = \min\{(1/2), (1/2)c_{m_l}\}$ and $\lambda_2 = \max\{(1/2), (1/2)c_{M_l}\}$. The motor controller and FES control input are discontinuous by design, therefore the time derivative of (30) exists almost everywhere (a.e.) within $t \in [t_0, \infty)$ and $\dot{V}(z) \stackrel{\text{a.e.}}{\in} \dot{V}(z)$, where \dot{V} is the generalized time derivative of (30). Let $z(t)$ for $t \in [t_0, \infty)$ be a Filippov solution to the differential inclusion $\dot{z} \in K[h](z)$, where $h: \mathbb{R}^3 \rightarrow \mathbb{R}^3$ is defined as $h \triangleq [\dot{e}_0 \quad \dot{e}_1 \quad \dot{r}]^T$ [38]. Solving (12)

for \dot{e}_0 and (13) for \dot{e}_1 , using (17), (19), (22), and (23), and canceling common terms produces

$$\begin{aligned} \dot{V} \leq & \chi r - B_M \sigma_s k_1 r^2 - B_{e_1} \sigma_e k_5 r^2 - \alpha_1 e_1^2 \\ & - \alpha_0 e_0^2 + e_0 e_1 - M_l M_{mc}^{-1} B_{e_{mc}} \sigma_{mc} k_9 r e_0 \\ & + M_l M_{mc}^{-1} B_{e_{mc}} \sigma_{mc} k_9 \alpha_0 r e_0 \\ & - B_M \sigma_s |r| (k_2 + k_3 \|z\| + k_4 \|z\|^2) \\ & - B_{e_1} \sigma_e |r| (k_6 + k_7 \|z\| + k_8 \|z\|^2). \end{aligned} \quad (32)$$

Proof: When $q_l \notin \mathcal{Q}_{FES}$, $\sigma_e = 1$ and $\sigma_s = 0$. Eliminating u_s , recognizing that $\sigma_{mc} \in \{0, 1\}$ for all time $t \in [t_n^e, t_n^s)$, and using Properties 1 and 7, (32) can be upper bounded by

$$\begin{aligned} \dot{V} \stackrel{\text{a.e.}}{\leq} & \|r\| (c_1 + c_2 \|z\| + c_3 \|z\|^2) \\ & - B_{e_1} k_5 r^2 - \alpha_1 e_1^2 - \alpha_0 e_0^2 + \|e_0\| \|e_1\| \\ & - B_{e_1} \|r\| (k_6 + k_7 \|z\| + k_8 \|z\|^2) \\ & + \frac{c_{M_l}}{c_{m_{mc}}} B_{e_{mc}} k_9 \|r\| (\|e_1\| + \alpha_0 \|e_0\|). \end{aligned}$$

Selecting the control gains as in (25) gives

$$\begin{aligned} \dot{V} \stackrel{\text{a.e.}}{\leq} & -B_{e_1} k_5 r^2 - \alpha_1 e_1^2 - \alpha_0 e_0^2 + \|e_0\| \|e_1\| \\ & + \frac{c_{M_l}}{c_{m_{mc}}} B_{e_{mc}} k_9 \|r\| (\|e_1\| + \alpha_0 \|e_0\|). \end{aligned}$$

Using Young's Inequality to upperbound the cross terms leads to

$$\begin{aligned} \dot{V} \stackrel{\text{a.e.}}{\leq} & -B_{e_1} k_5 r^2 - \alpha_1 e_1^2 - \alpha_0 e_0^2 + \frac{1}{2} (e_0^2 + e_1^2) \\ & + \frac{1}{2} \frac{c_{M_l}}{c_{m_{mc}}} B_{e_{mc}} k_9 [(1 + \alpha_0) r^2 + e_1^2 + \alpha_0 e_0^2]. \end{aligned}$$

Selecting the gains k_5, α_1, α_0 and k_9 as in (26)–(29), and defining $\psi_1 \triangleq k_5 - B_{e_{mc}} / (2B_{e_1}) (c_{M_l} / c_{m_{mc}}) k_9 (1 + \alpha_0)$, $\psi_2 \triangleq \alpha_1 - (1/2) (1 + (c_{M_l} / c_{m_{mc}}) B_{e_{mc}} k_9)$, and $\psi_3 \triangleq \alpha_0 - c_{m_{mc}} / (2c_{m_{mc}} - c_{M_l} B_{e_{mc}} k_9)$, then

$$\dot{V} \stackrel{\text{a.e.}}{\leq} -\psi_1 r^2 - \psi_2 e_1^2 - \psi_3 e_0^2 \quad (33)$$

is a negative definite function, where from (31) it can be shown that $\dot{V} \stackrel{\text{a.e.}}{\leq} -(\min(\psi_1, \psi_2, \psi_3)) / \lambda_2 V$. Solving the differential inequality for $\|z(t)\|$ and using (31) yields (24). From (30) and the resulting negative definite derivative in (33), $e_0, e_1, r \in \mathcal{L}_\infty, \forall t \in [t_n^e, t_n^s)$. Thus, the lower-body motor controller in (19), and master-cycle kinematic feedback controller in (22) are also shown to be bounded, such that $u_{e_l}, u_{e_{mc}} \in \mathcal{L}_\infty, \forall t \in [t_n^e, t_n^s)$, respectively. ■

Theorem 2: For $q_l \in \mathcal{Q}_{FES}$, where $t \in [t_n^s, t_{n+1}^e)$, the position and cadence error systems are globally exponentially stable in the sense that

$$\|z(t)\| \leq \sqrt{\frac{\lambda_2}{\lambda_1}} \|z(t_n^s)\| \exp\left[-\frac{\min(\psi_2, \psi_3, \psi_4)}{2\lambda_2} (t - t_n^s)\right] \quad (34)$$

provided the following gain conditions are met:

$$k_2 > \frac{c_1}{B_M}, \quad k_3 > \frac{c_2}{B_M}, \quad k_4 > \frac{c_3}{B_M} \quad (35)$$

$$k_1 > \frac{B_{e_{mc}}}{2B_M} \frac{c_{M_l}}{c_{m_{mc}}} k_9 (1 + \alpha_0) \quad (36)$$

as well as the gain conditions provided in (27)–(29), where ψ_4 is a known positive constant that can be adjusted through user defined control gains.

Proof: When $q_l \in \mathcal{Q}_{FES}$, $\sigma_e = \prod_{m \in \mathcal{M}} (1 - \beta_m \sigma_m)$ and $\sigma_s = 1$. Recognizing that $\sigma_{mc} \in (0, 1)$ for all time $t \in [t_n^s, t_{n+1}^e)$, and using Properties 1, 7, and 8, from (32) the time derivative of (30) can be upper bounded by

$$\begin{aligned} \dot{V} \stackrel{\text{a.e.}}{\leq} & \|r\| (c_1 + c_2 \|z\| + c_3 \|z\|^2) - B_M k_1 r^2 \\ & - B_{e_1} \sigma_e k_5 r^2 - \alpha_1 e_1^2 - \alpha_0 e_0^2 + \|e_0\| \|e_1\| \\ & - B_M \|r\| (k_2 + k_3 \|z\| + k_4 \|z\|^2) \\ & - B_{e_1} \sigma_e \|r\| (k_6 + k_7 \|z\| + k_8 \|z\|^2) \\ & + \frac{c_{M_l}}{c_{m_{mc}}} B_{e_{mc}} k_9 \|r\| (\|e_1\| + \alpha_0 \|e_0\|). \end{aligned}$$

Choosing the control gains as in (35) and recognizing that $0 \leq \sigma_e \leq 1$ gives

$$\begin{aligned} \dot{V} \stackrel{\text{a.e.}}{\leq} & -B_M k_1 r^2 - \alpha_1 e_1^2 - \alpha_0 e_0^2 + \|e_0\| \|e_1\| \\ & + \frac{c_{M_l}}{c_{m_{mc}}} B_{e_{mc}} k_9 \|r\| (\|e_1\| + \alpha_0 \|e_0\|). \end{aligned}$$

Selecting the gains α_1, α_0, k_9 as in (27)–(29) and k_1 as in (36), using Young's inequality as before, and defining $\psi_4 \triangleq k_1 - B_{e_{mc}} / (2B_{e_1}) (c_{M_l} / c_{m_{mc}}) k_9 (1 + \alpha_0)$, then

$$\dot{V} \stackrel{\text{a.e.}}{\leq} -\psi_4 r^2 - \psi_2 e_1^2 - \psi_3 e_0^2 \quad (37)$$

is a negative definite function, where from (31) it can be shown that $\dot{V} \stackrel{\text{a.e.}}{\leq} -(\min(\psi_2, \psi_3, \psi_4)) / \lambda_2 V$. From (30) and the resulting negative definite derivative in (37), $e_0, e_1, r \in \mathcal{L}_\infty, \forall t \in [t_n^s, t_{n+1}^e)$. Thus, the FES controller in (17), lower-body motor controller in (19), and master-cycle kinematic feedback controller in (22) are also shown to be bounded, such that $u_s, u_{e_l}, u_{e_{mc}} \in \mathcal{L}_\infty, \forall t \in [t_n^s, t_{n+1}^e)$, respectively. ■

Corollary 1: From Theorems 1 and 2, the combined lower-body rehabilitation cycle and master-cycle system produces global exponential tracking to the desired trajectory for all time t in the sense that

$$\|z(t)\| \leq \sqrt{\frac{\lambda_2}{\lambda_1}} \|z(t_0)\| \exp\left[-\frac{\zeta}{2\lambda_2} (t - t_0)\right] \quad (38)$$

where $\zeta \triangleq \min(\psi_1, \psi_2, \psi_3, \psi_4)$.

Proof: From (31), (33) and (37), and solving the resulting differential inequality, yields

$$\begin{aligned} \dot{V} \stackrel{\text{a.e.}}{\leq} & -\zeta \|z(t)\|^2 \stackrel{\text{a.e.}}{\leq} -\frac{\zeta}{\lambda_2} V \\ V(t) & \leq V(t_0) \exp\left[-\frac{\zeta}{\lambda_2} (t - t_0)\right]. \end{aligned} \quad (39)$$

Using (31) and solving the differential inequality in (39) for $\|z(t)\|$, yields (38). Recalling that $z \triangleq [e_0 \ e_1 \ r]^T$, $|e_0|, |e_1|, |r| \leq (\lambda_2 / \lambda_1)^{1/2} \|z(t_0)\| \exp[-\zeta / (2\lambda_2) (t - t_0)], \forall t$. From (17), (19), and (22), $u_s, u_{e_l}, u_{e_{mc}} \in \mathcal{L}_\infty$, for all time t . ■

V. EXPERIMENTS

To validate the developed master-cycle position and cadence tracking control system, experiments were performed on two sets of five non-disabled participants using two types of master-cycles.⁴ The first master-cycle type is a single-crank motorized recumbent lower-body cycle, representing the telerehabilitation use case, where a separate operator sets the desired trajectory using the master-cycle, and where the system parameters are similar to those of the split-crank rehabilitative cycle. The second type considered is a motorized hand-cycle, representing the rehab-by-wire use case, where the rehabilitation participant used their right hand to set the desired trajectory of the system. All of the FES control inputs are pulsewidth modulation forms of (17) along with the motor current input in (19) for the motor that produces torque about the lower-body crank shaft, and the master-cycle motor current input in (22) is used to provide resistive kinematic feedback to the master-cycle operator.

A. Experimental Testbed

The experimental testbed for the lower-body rehabilitation cycle consisted of a stationary TerraTrike Rover recumbent tricycle with a modified split-crank design similar to the testbed in [36]. The telerehabilitation system shown in Fig. 1 consisted of a similar TerraTrike Rover recumbent tricycle with a standard single-crank design. Both TerraTrike cycles have been modified to include a 300 W, 24 V brushed dc motor for each crank set. The rehab-by-wire system shown in Fig. 2 consisted of a hand-cycle coupled to a 150 W 24 V brushed dc motor. The position and cadence for the lower-body and master-cycle crank sets were measured using 20 000 pulses per revolution using US digital H1 encoders. A second-order low-pass filter and a 0.5 s moving average filter were applied across the master-cycle cadence data to reduce sensor noise and limit the effects of unintentional movement by the human master-cycle operator (i.e., muscle twitches, etc.) on desired trajectories. All motors were current-controlled using advanced motions controls (AMCs) motor drivers and power supplies. A Rehasim stimulator by Hasomed was used to deliver bi-phasic, rectangular, and symmetric pulses at a constant frequency of 60 Hz and a constant current of 90, 80, and 70 mA to the quadriceps, hamstrings, and gluteals, respectively. The encoders, motors, and stimulator were interfaced at a 1000-Hz sampling rate using a Quanser Q-PIDe DAQ connected to a Windows-based desktop computer running MATLAB with Simulink using the Real-Time Workshop. An emergency cut-off switch was installed on both cycles to ensure participant safety.

B. Experimental Methods

Experiments were performed on five non-disabled participants for each type of master-cycle with the demographics summarized in Table I, where each participant was assigned an identifying number. Prior to participation, written informed

⁴To reduce the possibility of COVID-19 transmission to vulnerable populations, testing for this validation experiment was limited to non-disabled participants.

TABLE I
PARTICIPANT DEMOGRAPHICS

	Participant	Age	Sex	Side Stimulated
Telerehabilitation	1T	23	F	Right
	2T	24	F	Right
	3T	29	M	Right
	4T	21	F	Right
	5T	23	F	Right
Rehab-by-wire	1R	23	F	Right
	2R	24	F	Right
	3R	21	F	Right
	4R	49	M	Right
	5R	25	M	Right

consent approved by the UF Institutional Review Board was provided (IRB202001554). Experiments were performed without volitional muscle effort by the participant to simulate a spinal cord injury causing a complete inability to pedal volitionally.

Axelgaard ValuTrode CF7515 electrodes were placed over each muscle group (i.e., quadriceps, gluteal, and hamstrings), then the participant's feet were secured to the crank set pedals using Össur Rebound Air Tall orthotic boots. The cycle's seat position was adjusted for participant comfort and to ensure that the knees maintained a minimum bend of at least 15°. Constant parameter measurements (i.e., seat position, limb length, etc.) were taken according to [16] to determine the participant's optimal muscle contraction regions (i.e., Q_m) to produce forward pedaling. A FES pulse width comfort limit was determined for each muscle group by running the cycle using motor effort only at 45 revolutions per minute (RPM) and then applying slowly increasing open-loop stimulation to individual muscle groups until the testing participant indicated that their comfort limit was reached for each muscle group. During experiments, in the case where the desired stimulation input to a given muscle reached the participant's set comfort limit, the applied FES input was saturated at the aforementioned limit.

For the telerehabilitation case (denoted by Case T) and the rehab-by-wire case (denoted by Case R), the experimental protocol used the motor controller in (19) to track the position and cadence of the master-cycle system over a period of 180 s. The FES controller in (17) was only active above a desired minimum cadence for stimulation of 30 RPM. Experimental results are referred to by the participant number followed by the use case (i.e., 1T denotes the experiment conducted with participant 1 using the teleoperation case).

VI. RESULTS

A. Lower-Body Tracking of the Master-Cycle Trajectory

Experimental results for the telerehabilitation (Fig. 1) and rehab-by-wire (Fig. 2) master-cycle use cases are presented in Table II. The average rms position errors were 4.98° and 7.31° for Case T and Case R, respectively. However, the average desired cadence for Case T set by the master-cycle was 49.52 RPM, and the average desired cadence for Case R was 52.81 RPM. Therefore, to provide a more accurate

TABLE II
POSITION AND CADENCE RESULTS FOR THE TELEREHABILITATION AND REHAB-BY-WIRE SYSTEMS*

Case	Participant	Position Error \dot{e}_0 (deg)	Peak Pos. Error \dot{e}_0 (deg)	Cadence Error $\dot{q}_{mc} - \dot{q}$ (RPM)	Peak Cad. Error $\dot{q}_{mc} - \dot{q}$ (RPM)	Avg. Des. Cadence \dot{q}_{mc} (RPM)	% Pos. Error Std. [†]	% Pos. Peak Error [†]	% Cad. Error Std.	% Cad. Peak Error
T	1T	-0.04±5.40	14.36	0.06±4.25	8.61	52.89±1.92	1.70	4.53	8.03	16.27
	2T	-0.04±4.68	10.96	0.05±3.21	7.72	52.67±1.87	1.48	3.47	6.09	14.65
	3T	0.01±8.00	20.99	0.05±6.17	9.97	49.37±1.28	2.70	7.08	12.51	20.20
	4T	-0.02±2.98	9.49	0.03±2.35	4.86	46.03±1.51	1.08	3.43	5.11	10.55
	5T	0.01±2.98	10.26	0.02±2.40	6.33	46.64±2.31	1.06	3.67	5.15	13.58
	Average	-0.02±4.80	13.21	0.04±3.68	7.50	49.52±1.78	1.61	4.44	7.38	15.05
R	1R	-0.19±7.48	18.92	-0.02±4.64	19.33	48.53±5.75	2.57	6.50	9.56	39.84
	2R	0.02±7.77	21.53	-0.01±3.17	11.31	50.02±6.60	2.59	7.17	6.34	22.61
	3R	0.82±7.08	32.98	-0.03±4.57	15.07	62.82±6.08	1.88	8.75	7.27	23.99
	4R	-0.03±5.88	14.87	-0.01±2.63	8.51	49.29±4.99	1.99	5.03	5.33	17.26
	5R	-0.13±7.40	28.51	-0.03±4.07	18.86	53.38±5.34	2.31	8.90	7.63	35.34
	Average	-0.10±7.12	23.36	-0.02±3.81	14.62	52.81±5.75	2.27	7.27	7.22	27.81

*Reported values were calculated during steady-state performance (i.e., after a 20 sec transient phase).

[†]Calculated relative to the mean value of master-cycle cadence converted to deg/sec.

^{||}Calculated relative to the mean value of master-cycle cadence given in RPM.

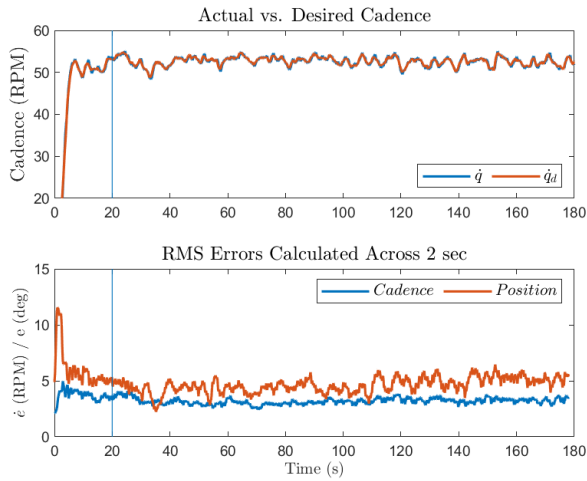


Fig. 3. Participant 2T: The actual versus desired telerehabilitation cadence and the resulting rms cadence error (RPM) and position error (degree), where the average steady-state desired cadence was 52.67 ± 1.87 RPM. For visual clarity, a moving average filter across 600 data points was applied to the cadence. The 20 s transient period is indicated by the vertical blue line.

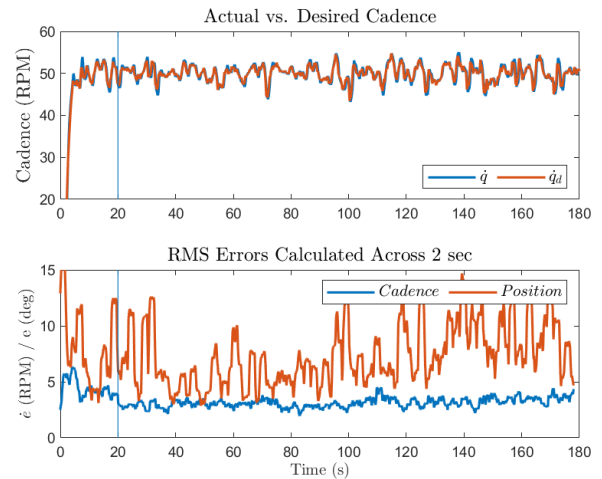


Fig. 4. Participant 2R: The actual versus desired rehab-by-wire cadence and the resulting rms cadence error (RPM) and position error (degree), where the average steady-state desired cadence was 50.02 ± 6.60 RPM. For visual clarity, a moving average filter across 600 data points was applied to the cadence. The 20 s transient period is indicated by the vertical blue line.

representation of the results, the average rms position errors were normalized using their respective average cadence (converted to degree/s) and found to be 1.68% of the average cadence for Case T and 2.31% for Case R. The average rms cadence error was 3.67 RPM for Case T and 3.87 RPM for Case R, which represents 7.41% and 7.34% of the average cadences, respectively. An example of the desired versus actual cadence values, as well as the rms errors of the cadence and angular position for Participant 2T with a teleoperated master-cycle are shown in Fig. 3, while the same comparisons for Participant 2R are included in Fig. 4. It is concluded that the developed controllers are capable of producing similar trajectory tracking results despite an unpredictable, variable desired cadence. Furthermore, when compared to the average position tracking result of $-6.93^\circ \pm 8.78^\circ$ for non-disabled participants using a split-crank cycle in [34], the developed controller eliminates the consistent error offset and results in

average tracking errors of $-0.02^\circ \pm 4.80^\circ$ and $-0.10^\circ \pm 7.12^\circ$ given the variable cadences produced by Case T and Case R, respectively.

B. FES Pulsewidth, Angular Position Error, and Motor Effort

A 10 s representation of the FES control input u_s , lower-body electric motor current u_{el} , and angular position error \dot{e}_0 for Participant 2T is provided in Fig. 5 and 2R is provided in Fig. 6.⁵ By inspection of Fig. 5, it is shown that for Participant 2T, the developed controller significantly reduces the motor effort within the quadriceps region while a small reduction of motor effort occurs in the hamstring region due to the selected

⁵Participant 2T and 2R are the same rider who participated on separate days to evaluate both use cases. Therefore, the control gains were the same values in both cases. Specifically, $\alpha_0 = 0.9$, $\alpha_1 = 1.8$, $k_1 = 25$, $k_2 = 0.05$, $k_3 = 0.05$, $k_4 = 0.005$, $k_5 = 15$, $k_6 = 0.05$, $k_7 = 0.05$, and $k_8 = 0.05$.

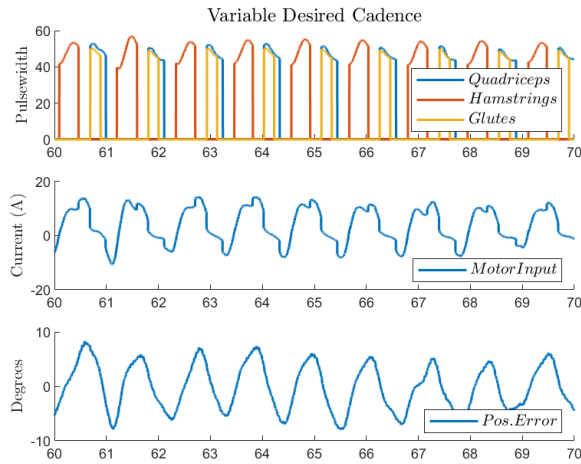


Fig. 5. Data shown is for Participant 2T. The follower-cycle performance of the FES pulsewidth (i.e., FES control input) at top, lower-body electric motor current in the middle, and angular position error at the bottom.

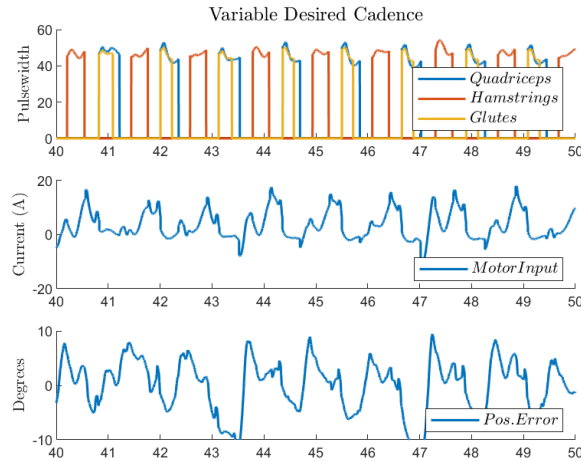


Fig. 6. Data shown is for Participant 2R. The follower-cycle performance of the FES pulsewidth (i.e., FES control input) at top, lower-body electric motor current in the middle, and angular position error at the bottom.

motor assistance terms $\beta_Q = 0.8$, $\beta_H = 0.2$, and $\beta_G = 0$, as defined in (20). This result is less clear for Participant 2R in Fig. 6 despite using the same motor assistance terms (i.e., β terms) as participant 2T. Here the rehab-by-wire system appears to produce higher frequency variance in the electric motor current u_{e_i} and angular position error \dot{e}_0 , seen clearly at approximately 43.5 s where the position error makes a 20° shift leading to a corresponding shift in motor effort.

C. Kinematic Feedback

A 10 s representation of the telerehabilitation master-cycle motor input $u_{e_{mc}}$ for Participant 2T is depicted in Fig. 7 and 2R is depicted in Fig. 8, where the electric motor effort is directly proportional to the lower-body position error when the switching condition σ_{mc} is met. The motor effort is applied to resist the master-cycle operator when the position error grows in the same direction as the cadence, assisting with lower-body position tracking given a sufficient control gain k_θ . As shown in Fig. 8, resistive motor torque is applied at the hand-cycle in direct response to the rapid shift in position error that occurs

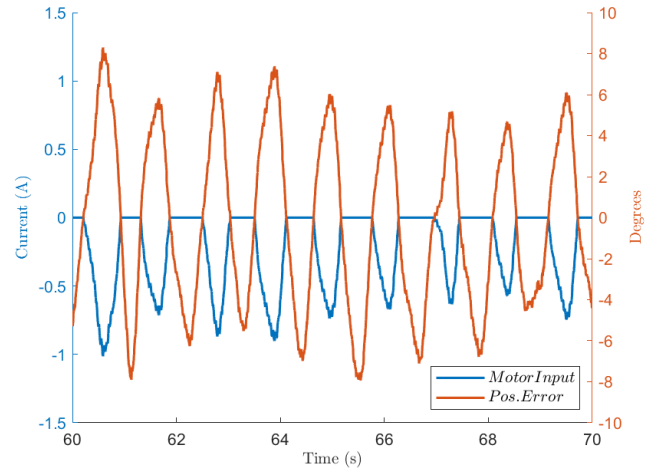


Fig. 7. Data shown is for Participant 2T. The telerehabilitation master-cycle electric motor current is shown in relation to the lower-body position error across a 10 s period, where the motor is only active when the switching condition σ_{mc} is met.

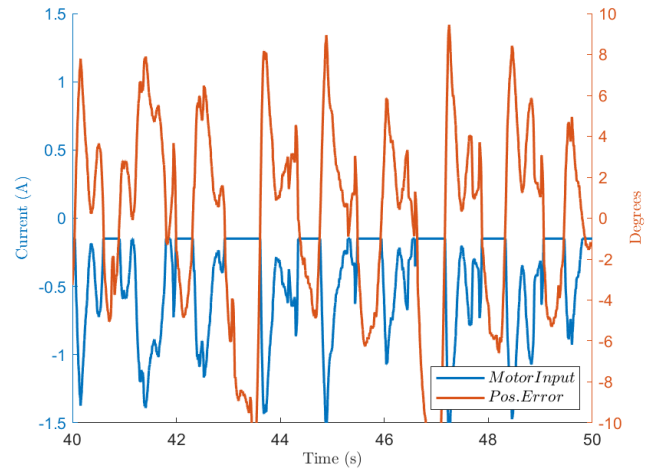


Fig. 8. Data shown is for Participant 2R. The rehab-by-wire master-cycle electric motor current is shown in relation to the lower-body position error across a 10 s period, where the motor is only active when the switching condition σ_{mc} is met.

at approximately 43.5 s, resulting in a reduction of position error.

VII. DISCUSSION

To show the efficacy of the developed strategy, empirical gain tuning methods were used. This approach led to gain values which proved to be robust across all participants, where slight adjustments were motivated by factors such as participant comfort and muscle reactivity.

It should be noted that recent work by Alibeji et al. [28] provides an important inroad to compensate for communication delay within a FES enabled bilateral telerehabilitation system, where a stability analysis indicates a globally uniformly ultimately bounded result. In their development, the error signals e_r and e_s are designed to track the delayed trajectories of the corresponding systems. A similar method could be used to modify (11)–(13), yielding similar stability results. Future work will explore the result presented in [28], as well as methods designed to predict actual trajectories

from delayed signals, for application to the high-velocity FES telerehabilitation cycle presented in this work.

The purpose of this current work was to develop a control strategy for low-cost, in-home FES-enabled telerehabilitation and rehab-by-wire systems. Some Lyapunov-based control methods, such as recurrent or repetitive learning, would be ill-suited due to the existence of user-generated desired trajectories. Instead, Lyapunov-based robust sliding-mode controllers were developed for their ability to provide global exponential tracking results at a relatively low computational cost. RISE-based controllers [39], [40] could likely be used to provide a continuous control alternative to sliding mode control while still yielding the same stability result. High-gain robust control methods could also be used, but would likely yield a uniformly ultimately bounded result. Adaptive control methods are an area of future investigation, given the potential for lower frequency and reduced magnitude compensation; however, adaptive control can be challenging to apply for additive exogenous disturbances (e.g., the disturbance does not have a linear in the parameters structure and time does not lie on a compact domain, yielding challenges for methods such as neural networks).

VIII. CONCLUSION

In comparison to the teleoperation case, the rehab-by-wire case, where the desired trajectory was set by a hand-cycle manipulated by the rehabilitation participant, the resulting position errors increased to 6.91% of the average desired cadence. This result is likely due to a substantial difference in parameter values between the hand-cycle system and the FES/motor-actuated split-crank cycle. Relatively low internal friction and damping in the hand-cycle lead to an average standard deviation in position error of 7.12° compared to only 4.80° when a recumbent cycle set the desired cadence, which ultimately led to an average peak position errors of 23.36° and 13.21° when the desired cadence was set by the hand-cycle (i.e., Case R) and the recumbent cycle (i.e., Case T), respectively. It is theorized that these physical differences in the respective mechanical systems also explain the high-frequency variance depicted in Figs. 4, 6, and 8.

Despite these performance differences between the two tested types of master-cycle systems, the developed controller produced an average position tracking error (calculated across both types of master-cycle) of $0.04^\circ \pm 5.96^\circ$ compared to the prior result from Rouse, et. al. of $-6.93^\circ \pm 8.78^\circ$ for non-disabled participants tracking a constant-cadence trajectory using a split-crank cycle [34]. Thus, the developed controller, with the inclusion of an integral position error and variable motor assistance, eliminates the undesirable steady-state offset and reduces the standard deviation of position error that has been reported in other works, despite tracking a teleoperated variable-cadence trajectory. Furthermore, the motor and FES muscle controllers result in global exponential tracking to a user-controlled variable-cadence desired trajectory despite high-velocity operation. This development provides an inroad for future telerehabilitation and rehab-by-wire applications.

Future work could include the development of new controllers for the master-cycle system to simulate desirable

dynamic properties, such as friction, inertial, and applied force terms. These terms might then be used to mimic the properties of known systems, leading to enhanced feedback to the master-cycle operator and improved position tracking despite differences between the master-cycle and follower-cycle mechanical parameters. Furthermore, the use of surface electromyography (sEMG) and ultrasound imaging, as in [41], could be used to help predict expected torque values at the crank arm, leading to online adaptation of required motor assistance. The predicted torque values could also be beneficial for providing informed haptic feedback to the master-cycle system. Extended clinical trials would be beneficial for evaluating the effectiveness of the resulting paired positions of the corresponding upper and lower limbs produced during the rehab-by-wire use case for the restoration of motor function and improved neuroplasticity. Finally, communication delay is an additional significant challenge for telerehabilitation. While the result in [28] provides an inroad, alternative methods are also motivated.

ACKNOWLEDGMENT

Any opinions, findings and conclusions or recommendations expressed in this material are those of the author(s) and do not necessarily reflect the views of the sponsoring agency.

REFERENCES

- [1] A. Bersano et al., "Stroke care during the COVID-19 pandemic: Experience from three large European countries," *Eur. J. Neurol.*, vol. 27, no. 9, pp. 1794–1800, Sep. 2020.
- [2] R. Berkelmans, "Fes cycling," *J. Autom. Control*, vol. 18, no. 2, pp. 73–76, 2008.
- [3] A. Kralj and T. Bajd, *Functional Electrical Stimulation: Standing and Walking After Spinal Cord Injury*. Boca Raton, FL, USA: CRC Press, 1989.
- [4] M. Bélanger, R. B. Stein, G. D. Wheeler, T. Gordon, and B. Leduc, "Electrical stimulation: Can it increase muscle strength and reverse osteopenia in spinal cord injured individuals?" *Arch. Phys. Med. Rehabil.*, vol. 81, no. 8, pp. 1090–1098, Aug. 2000.
- [5] M. M. Rodgers et al., "Musculoskeletal responses of spinal cord injured individuals to functional neuromuscular stimulation-induced knee extension exercise training," *J. Rehabil. Res. Develop.*, vol. 28, no. 4, pp. 19–26, 1991.
- [6] S. P. Hooker et al., "Physiologic effects of electrical stimulation leg cycle exercise training in spinal cord injured persons," *Arch. Phys. Med. Rehabil.*, vol. 73, no. 5, pp. 470–476, 1992.
- [7] T. Mohr, J. Pødenphant, F. Biering-Sørensen, H. Galbo, G. Thamsborg, and M. Kjaer, "Increased bone mineral density after prolonged electrically induced cycle training of paralyzed limbs in spinal cord injured man," *Calcified Tissue Int.*, vol. 61, no. 1, pp. 22–25, Jul. 1997.
- [8] T. Yan, C. W. Y. Hui-Chan, and L. S. W. Li, "Functional electrical stimulation improves motor recovery of the lower extremity and walking ability of subjects with first acute stroke: A randomized placebo-controlled trial," *Stroke*, vol. 36, no. 1, pp. 80–85, Jan. 2005.
- [9] S. Ferrante, A. Pedrocchi, G. Ferrigno, and F. Molteni, "Cycling induced by functional electrical stimulation improves the muscular strength and the motor control of individuals with post-acute stroke," *Eur. J. Phys. Rehabil. Med.*, vol. 44, no. 2, pp. 159–167, 2008.
- [10] F. Molteni, G. Gasperini, G. Cannaviello, and E. Guanziroli, "Exoskeleton and end-effector robots for upper and lower limbs rehabilitation: Narrative review," *Phys. Med. Rehab.*, vol. 10, no. 9, pp. 174–188, 2018.
- [11] G. Morone et al., "Robot-assisted gait training for stroke patients: Current state of the art and perspectives of robotics," *Neuropsychiatric Disease Treatment*, vol. 13, pp. 1303–1311, May 2017.
- [12] M. F. Bruni, C. Melegari, M. C. De Cola, A. Bramanti, P. Bramanti, and R. S. Calabro, "What does best evidence tell us about robotic gait rehabilitation in stroke patients: A systematic review and meta-analysis," *J. Clin. Neurosci.*, vol. 48, pp. 11–17, Feb. 2018.

- [13] E. J. Plautz, G. W. Milliken, and R. J. Nudo, "Effects of repetitive motor training on movement representations in adult squirrel monkeys: Role of use versus learning," *Neurobiol. Learn. Memory*, vol. 74, no. 1, pp. 27–55, Jul. 2000.
- [14] M. O. Krucoff, S. Rahimpour, M. W. Slutzky, V. R. Edgerton, and D. A. Turner, "Enhancing nervous system recovery through neurobiologics, neural interface training, and neurorehabilitation," *Frontiers Neurosci.*, vol. 10, p. 584, Dec. 2016.
- [15] C. Cousin, V. Duenas, and W. E. Dixon, "FES cycling and closed-loop feedback control for rehabilitative human–robot interaction," *Robotics*, vol. 10, no. 61, pp. 1–23, 2021.
- [16] M. J. Bellman, R. J. Downey, A. Parikh, and W. E. Dixon, "Automatic control of cycling induced by functional electrical stimulation with electric motor assistance," *IEEE Trans. Autom. Sci. Eng.*, vol. 14, no. 2, pp. 1225–1234, Apr. 2017.
- [17] T. Klarner, T. S. Barss, Y. Sun, C. Kaupp, P. M. Loadman, and E. P. Zehr, "Exploiting interlimb arm and leg connections for walking rehabilitation: A training intervention in stroke," *Neural Plasticity*, vol. 2016, pp. 1–19, Jan. 2016.
- [18] D. P. Ferris, H. J. Huang, and P.-C. Kao, "Moving the arms to activate the legs," *Exercise Sport Sci. Rev.*, vol. 34, no. 3, pp. 113–120, Jul. 2006.
- [19] R. Zhou, L. Alvarado, R. Ogilvie, S. L. Chong, O. Shaw, and V. K. Mushahwar, "Non-gait-specific intervention for the rehabilitation of walking after SCI: Role of the arms," *J. Neurophysiol.*, vol. 119, no. 6, pp. 2194–2211, Jun. 2018.
- [20] N. Lehrer, S. Attygalle, S. L. Wolf, and T. Rikakis, "Exploring the bases for a mixed reality stroke rehabilitation system, part I: A unified approach for representing action, quantitative evaluation, and interactive feedback," *J. NeuroEng. Rehabil.*, vol. 8, no. 1, pp. 1–51, 2011.
- [21] M. W. O'Dell, C.-C.-D. Lin, and V. Harrison, "Stroke rehabilitation: Strategies to enhance motor recovery," *Annu. Rev. Med.*, vol. 60, no. 1, pp. 55–68, Feb. 2009.
- [22] M. Minge, E. Ivanova, K. Lorenz, G. Joost, M. Thuring, and J. Kruger, "BeMobil: Developing a user-friendly and motivating telerehabilitation system for motor relearning after stroke," in *Proc. Int. Conf. Rehabil. Robot. (ICORR)*, Jul. 2017, pp. 870–875.
- [23] M. H. Lee, "A technology for computer-assisted stroke rehabilitation," in *Proc. 23rd Int. Conf. Intell. User Interfaces*, Mar. 2018, pp. 665–666.
- [24] R. F. Polak, A. Bistrisky, Y. Gozlan, and S. Levy-Tzedek, "Novel gamified system for post-stroke upper-limb rehabilitation using a social robot: Focus groups of expert clinicians," in *Proc. Int. Conf. Virtual Rehabil. (ICVR)*, Jul. 2019, pp. 1–7.
- [25] M. Mendoza, I. Bonilla, E. González-Galván, and F. Reyes, "Impedance control in a wave-based teleoperator for rehabilitation motor therapies assisted by robots," *Comput. Methods Programs Biomed.*, vol. 123, pp. 54–67, Jan. 2016.
- [26] M. D. Duong, C. Teraoka, T. Imamura, T. Miyoshi, and K. Terashima, "Master-slave system with teleoperation for rehabilitation," in *Proc. 16th Triennial World Congr.*, 2005, vol. 38, no. 1, pp. 48–53.
- [27] N. Norouzi-Gheidari, P. S. Archambault, and J. Fung, "Effects of robot-assisted therapy on stroke rehabilitation in upper limbs: Systematic review and meta-analysis of the literature," *J. Rehabil. Res. Develop.*, vol. 49, no. 4, pp. 479–496, 2012.
- [28] N. Alibeji, B. E. Dicianno, and N. Sharma, "Bilateral control of functional electrical stimulation and robotics-based telerehabilitation," *Int. J. Intell. Robot. Appl.*, vol. 1, no. 1, pp. 6–18, Feb. 2017.
- [29] N. A. Stanton and P. Marsden, "From fly-by-wire to drive-by-wire: Safety implications of automation in vehicles," *Saf. Sci.*, vol. 24, no. 1, pp. 35–49, Oct. 1996.
- [30] Y.-J. Pan, C. Canudas-de-Wit, and O. Sename, "A new predictive approach for bilateral teleoperation with applications to drive-by-wire systems," *IEEE Trans. Robot.*, vol. 22, no. 6, pp. 1146–1162, Dec. 2006.
- [31] C.-H. Wu, W.-C. Lin, and K.-S. Wang, "Mechatronics and remote driving control of the drive-by-wire for a go kart," *Sensors*, vol. 20, no. 4, p. 1216, 2020. [Online]. Available: <https://www.mdpi.com/1424-8220/20/4/1216>
- [32] K. Stubbs, B. C. Allen, and W. E. Dixon, "Teleoperated motorized functional electric stimulation actuated rehabilitative cycling," in *Proc. ASME Dyn. Syst. Control Conf.*, 2020, pp. 1–8.
- [33] F. I. E. Estay, C. A. Rouse, M. H. Cohen, C. A. Cousin, and W. E. Dixon, "Cadence and position tracking for decoupled legs during switched split-crank motorized FES-cycling," in *Proc. Amer. Control Conf. (ACC)*, Jul. 2019, pp. 854–859.
- [34] C. A. Rouse, C. A. Cousin, B. C. Allen, and W. E. Dixon, "Shared control for switched motorized FES-cycling on a split-crank cycle accounting for muscle control input saturation," *Automatica*, vol. 123, Jan. 2021, Art. no. 109294.
- [35] C. A. Rouse, C. A. Cousin, B. C. Allen, and W. E. Dixon, "Split-crank cadence tracking for switched motorized FES-cycling with volitional pedaling," in *Proc. Amer. Control Conf. (ACC)*, Jul. 2019, pp. 4393–4398.
- [36] C. A. Rouse, C. A. Cousin, V. H. Duenas, and W. E. Dixon, "Cadence tracking for switched FES cycling combined with voluntary pedaling and motor resistance," in *Proc. Annu. Amer. Control Conf. (ACC)*, Jun. 2018, pp. 4558–4563.
- [37] M. Ferre, M. Buss, R. Aracil, C. Melchiorri, and C. Balaguer, *Advances in Telerobotics*, B. Siciliano, O. Khatib, and F. Groen, Eds. Berlin, Germany: Springer, 2007.
- [38] N. Fischer, R. Kamalapurkar, and W. E. Dixon, "LaSalle-yoshizawa corollaries for nonsmooth systems," *IEEE Trans. Autom. Control*, vol. 58, no. 9, pp. 2333–2338, Sep. 2013.
- [39] P. M. Patre, W. MacKunis, K. Dupree, and W. E. Dixon, "Modular adaptive control of uncertain Euler–Lagrange systems with additive disturbances," *IEEE Trans. Autom. Control*, vol. 56, no. 1, pp. 155–160, Jan. 2011.
- [40] O. S. Patil, A. Isaly, B. Xian, and W. E. Dixon, "Exponential stability with RISE controllers," *IEEE Control Syst. Lett.*, vol. 6, pp. 1592–1597, 2022.
- [41] Q. Zhang, N. Fragnito, J. R. Franz, and N. Sharma, "Fused ultrasound and electromyography-driven neuromuscular model to improve plantarflexion moment prediction across walking speeds," *J. NeuroEng. Rehabil.*, vol. 19, no. 1, p. 86, Aug. 2022.



Kimberly J. Stubbs received the M.Sc. degree from the Department of Mechanical and Aerospace Engineering, University of Florida, Gainesville, FL, USA, in 2021, where she is currently pursuing the Ph.D. degree.

Her main research interests include the application of Lyapunov-based control techniques for uncertain nonlinear systems, with a focus on rehabilitation robotics and physical human-machine interaction.



Brendon C. Allen (Member, IEEE) received the Ph.D. degree from the Department of Mechanical and Aerospace Engineering, University of Florida, Gainesville, FL, USA, in 2021.

He joined the Department of Mechanical Engineering, Auburn University, Auburn, AL, USA, in 2021. His main research interests include the development of robust, adaptive, or learning Lyapunov-based control techniques for uncertain nonlinear systems such as: rehabilitation robotics, autonomous systems, and switched/hybrid systems.



Warren E. Dixon (Fellow, IEEE) received the Ph.D. degree in electrical engineering from Clemson University, Clemson, SC, USA, in 2000.

After working as a Wigner Fellow and a Research Staff Member at Oak Ridge National Laboratory, Oak Ridge, TN, USA. In 2004, he joined the University of Florida, Gainesville, FL, USA, where he is now the Dean's Leadership Professor and the Department Chair with the Department of Mechanical and Aerospace Engineering. His main research interest has been the development and application of Lyapunov-based control techniques for uncertain nonlinear systems.

Dr. Dixon work has been acknowledged by various Early and Mid-Career Awards and Best Paper Awards. He is an ASME Fellow for contributions to adaptive control of uncertain nonlinear systems.